ACS APPLIED MATERIALS & INTERFACES

RESEARCH ARTICLE

www.acsami.org

Solvent-Free Preparation of High-Toughness Epoxy−SWNT Composite Materials

Jose M. González-Domínguez,[†] Alejandro Ansón-Casaos,[†] Ana M. Díez-Pascual,[‡] Behnam Ashrafi,[§] Mohammed Naffakh,[‡] David Backman,[§] Hartmut Stadler,[⊥] Andrew Johnston,[§] Marian Gómez,[‡] and M. Teresa Martínez*[,†]

[†]Carbon Nanostructures and Nanotechnology Group, Instituto de Carboquímica, CSIC, c/Miguel Luesma Castan 4, 50018 Zaragoza, Spain

[‡]Department of Polymer Physics and Engineering, Instituto de Ciencia y Tecnología de Polímeros, CSIC, c/Juan de la Cierva 3, 28006 Madrid, Spain

[§]Institute for Aerospace Research, NRC, 1200 Montreal Road, Ottawa (Canada)

[⊥]Veeco Insturments GmbH, Dynamostrasse 19, D-68165, Manhein (Germany)

Supporting Information

ABSTRACT: Multicomponent nanocomposite materials based on a high-performance epoxy system and single-walled carbon nanotubes (SWNTs) have been prepared. The noncovalent wrapping of nitric acid-treated SWNTs with a PEO-based amphiphilic block copolymer leads to a highly disaggregated filler with a boosted miscibility in the epoxy matrix, allowing its dispersion without organic solvents. Although direct dispersion of acid-treated SWNTs results in modestly improved epoxy matrix mechanical properties, the incorporation of wrapped SWNTs produces a huge increase in toughness (276% improvement at 0.5 wt % loading) and impact strength (193% at 0.5 wt % loading) with no detrimental effect on the elastic properties. A synergistic effect between SWNTs and the block copolymer is revealed on the basis of tensile and impact strength results. Atomic force microscopy has been applied, obtaining stiffness mappings that identify nanostructure features responsible of the dynamic mechanical behavior. The electrical percolation threshold is greatly reduced, from 0.31 to 0.03 wt % SWNTs when block copolymer-wrapped SWNTs are used, and all the measured conductivity values increased up to a maximum of 7 orders of magnitude with respect to the baseline matrix (1 wt % wrapped-SWNTs loading). This approach provides an efficient way to disperse barely dispersible SWNTs without solvents into an epoxy matrix, and to generate substantial improvements with small amounts of SWNTs.

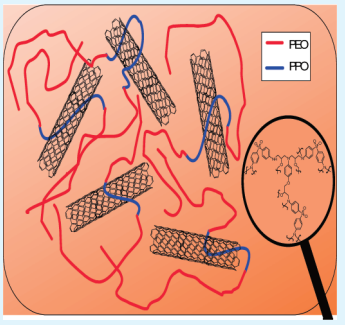

KEYWORDS: single-walled carbon nanotubes, epoxy nanocomposites, block copolymer, toughness, impact strength, electrical conductivity

1. INTRODUCTION

Epoxy resins are electrically insulating thermosetting materials widely used in structural applications because of their intrinsic stiffness, chemical, and heat resistance derived from a heavily cross-linked structure. The base material is brittle and often provides low wear resistance and low toughness that hinder use in most structural, adhesive, or coating applications. The need for toughening and tuning other physical properties of these materials arises from the requirement to adapt to a wide spectrum of potential applications. This is typically achieved by the addition of reinforcing and/or conductive fillers. For example, an epoxy resin can become conductive by adding silver particles, creating the potential for a conductive adhesive for electronic applications.

With the general goal of improving epoxy performance, reinforcement with nanoscale fillers currently represents an active field of research for advanced high-performance applications.

Carbon nanotubes, in particular the single-walled variety (SWNTs), have outstanding performance[1,2] and are low density, which is of critical interest in applications where the weight reduction is crucial, such as in the aircraft or automotive industries. Poor interfacial adhesion, lack of transfer of their properties, agglomeration and low uniformity of SWNT distribution are the biggest challenges when dealing with nanotube-reinforced polymer composites.[3] Achieving an optimum nanotubes dispersion and/or individualization in a nanocomposite material is of a great importance, since its final properties (e.g., mechanical or electrical performance) can be dramatically enhanced[4] and also because new features may arise, such as optical transparency,[5] which may provide unique applications to these materials.

The integration of SWNTs into an epoxy thermoset material is accomplished through blending with the epoxide precursor and/or the curing agent, followed by thermally-activated crosslinking reactions in the presence of SWNTs.[6] Mechanical treatments,

Received: December 22, 2010
Accepted: February 23, 2011
Published: April 15, 2011

such as high shear strains[7] or ultrasound[8] (generally in organic solvents[1,6]) are the most widely used integration methods, with variable results obtained. Moreover, the use of SWNTs has the added difficulty of achieving bundle exfoliation, which is not easily achieved using these methods. More recently, there has been a growing interest in chemical functionalization of SWNTs to improve integration and dispersion in epoxy resins.[1,3,6] One of the most notable pieces of work was reported by Zhu et al.[9] in which the combination of acid treatment and fluorination produced functionalized SWNTs that were successfully dispersed into a diglycidyl ether of bisphenol A (DGEBA)-based epoxy system by sonication in organic solvent. The filler exhibited more homogeneous distribution in the epoxy matrix as compared to unfunctionalized SWNTs. There have been other attempts to disperse carbon nanotubes into epoxy resins based on non-covalent wrapping. Commercial surfactants[10−14] or natural polymers (i.e., Gum Arabic,[15] proteins[16]) have been utilized with the aim of dispersing pristine or functionalized nanotubes in organic solvents prior to their integration. In general, functionalization (covalent or not) is pursued to increase the dispersibility of nanotubes in organic solvents in which sonication is carried out followed by evaporation and curing of the resulting epoxy blend. This enhanced solubility in organic media often provides temporarily stable nanotube dispersions, and the solvent evaporation process leads to inhomogeneous distributions when not done quickly enough.[3,17] Furthermore, the final properties of the nanocomposites can be compromised by the solvent traces remaining after evaporation.[18]

A non-covalent approach with block copolymers (BCs) has not been widely used in SWNT-reinforced epoxy resins, and has been limited to the use of Disperbyk-2150 dispersant.[19−21] Amphiphilic BCs have been shown to cause a toughening effect by self-assembled nanostructure formation in epoxy resins.[22,23] A judicious choice of the respective blocks allows selectively favoring their miscibility into the epoxy resin, causing the formation of different vesicular and micellar structures that are responsible for the toughening effect. On the other hand, this tunable lyophilicity difference between polymer blocks can be employed in liquid media to obtain highly dispersed SWNTs. Processing these dispersed SWNTs leads to powders with a high content of individual tubes.[24] Combining both effects provides a toughness improvement along with the advantages inherent to the integration of debundled SWNTs. Filler−matrix adhesion is also expected to improve, since the epoxyphobic block would possess more affinity for the SWNTs and thus interconnect them to the matrix throughout the epoxy-miscible block (Scheme 1).

In the present work, we have employed the aforementioned approach in order to achieve effective reinforcement in an aerospace-grade high performance epoxy system. We have used the ability of BCs to disperse and disentangle SWNTs thus producing highly debundled arc-discharge SWNTs wrapped by Pluronic F68 BC.[25] Improved dispersion into a trifunctional epoxy was demonstrated by means of differential scanning calorimetry studies of the curing reaction. The solubility of the Pluronic-wrapped SWNTs powders into the epoxy resin was so high that the dispersion could be carried out with a solvent-free method which included stirring and mild sonication stages. The as-manufactured nanocomposites have already demonstrated important improvements in thermo-oxidative stability of the parent epoxy matrix.[26] A complete and comprehensive study of these epoxy nanocomposite materials properties is presented in the present paper to assess the BC-wrapped SWNTs potential as epoxy matrix filler.

Scheme 1. Conceptual Visualization of the Dispersion Method Based on Pluronic Wrapping, With Highlight on the Matrix Chemical Cross-Linked Structure (elements not to scale)

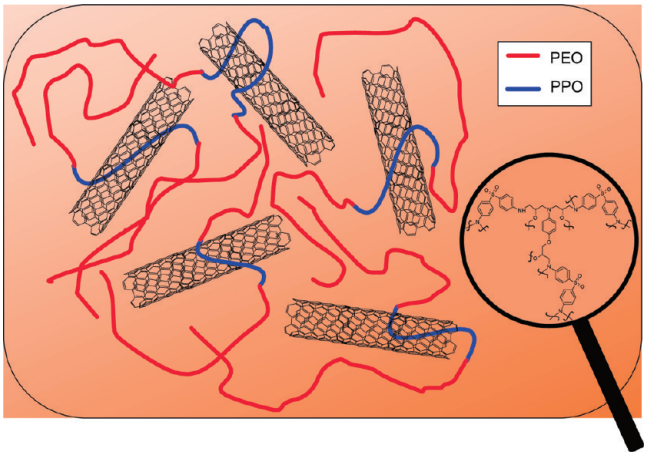

2. EXPERIMENTAL SECTION

Materials. The epoxy system studied in the present work consisted of a high-performance trifunctional epoxy, triglycidyl *p*-aminophenol (TGAP) with a 4,4′-diaminodiphenyl sulfone (DDS) curing agent. Both were kindly provided by the Huntsman Corporation. SWNTs were synthesized by the arc discharge method,[27] using Ni/Y catalyst mixture in a 2/0.5 atomic ratio. They were treated using a refluxing nitric acid treatment (1.5M, 2h), followed by centrifugation (10 000 rpm, 4 h), washing with deionised water, filtration, and drying. A complete characterization of this material is published elsewhere.[28] Treated SWNTs were subjected to a wrapping process in aqueous solution of Pluronic F68 BC using tip sonication, centrifugation and filtering. The detailed wrapping process in Pluronic F68 block copolymer can be found in reference,[25] along with the characterization method. The Pluronic-wrapped SWNTs had a final content in Pluronic of ∼30 wt %, as determined by thermogravimetric analysis. The SWNTs incorporated in TGAP + DDS epoxy system were bare acid-treated and Pluronic-wrapped respectively, for comparison. Raman spectra of pristine, acid-treated and Pluronic-wrapped SWNTs are shown in Figure S1 (Supporting Information).

Nanocomposites Preparation. Neat (TGAP + DDS) epoxy was prepared by directly blending TGAP and DDS in a stoichiometric functionality ratio (100/67) at 60°C for 15 min. Different nanocomposites containing 0.1, 0.25, 0.5, 1, and 2 wt % of Pluronic-wrapped or bare acid-treated SWNTs were prepared by a solvent-free method including hot stirring (at 60°C) and tip sonication.[25] The Epoxy + Pluronic blank samples were prepared by the same solvent-free procedure, mixing the neat resin with the same amounts of Pluronic present in each nanocomposite sample, according to the final Pluronic content in the wrapped SWNTs (0.03, 0.075, 0.15, 0.3, and 0.6 wt % respectively). For dynamic mechanical analysis (DMA) and electrical characterization the curing was performed as follows: the epoxy blend after the mixing protocol was cast into a steel dish mold sealed by teflon plates (3 mm thick), followed by curing at 200°C for 30 min in a Perkin Elmer hydraulic press coupled to a Greaseby Specac controlled heater, under 3 tones of pressure. The sample was removed from the mold, transferred to a Carbolite LHT4/30 oven and postcured at 200°C for 4h. For tensile

characterization dog-bone coupons were manufactured through liquid molding to dimensions required by ASTM D638[29] using a teflon mold placed inside an aluminum housing. Using a teflon tube, air pressure of 60-70 psi (483-551 KPa) was applied inside the mold to remove the air bubbles from the resin. Identical curing and postcuring conditions were employed for the dog-bone specimens manufacturing. The atomic force microscopy (AFM) samples were prepared by drop casting of the uncured epoxy blends on a glass substrate and subsequently cured in oven at 200°C for 4.5h.

Characterization Techniques. Optical microscopy images were collected with a Zeiss AXIO optical microscope, coupled to a Cannon digital camera, in order to observe epoxy/SWCNT blends at 50× magnification. A small drop of the epoxy blend was cast on a glass slide and covered with a 0.5 mm thin glass cover prior to the observation.

Scanning electron microscopy (SEM) experiments were made in a scanning electron microscope (Hitachi S3400N), working in the secondary electrons mode at a high voltage 15 kV and a distance of 5 mm. Cured samples were fractured and the edge was sputtered with a 10 nm gold layer prior to their observation.

Transmission electron microscopy (TEM) images were taken with a JEOL-2000 FXII electron microscope, working at 200 kV and with 0.28 nm point-to-point resolution. Cured samples were cut using a microtome and deposited on a copper grid for their further use.

DMA tests were carried out using a Mettler DMA 861 dynamic mechanical analyzer, in tensile mode at frequencies of 0.1, 1, and 10 Hz. The specimen dimensions were ~19.5 × 5 × 2 mm^3, obtained by cutting bigger test samples with a diamond circular saw. Measurements were performed from −100 °C to the temperature at which the specimens became unable to be tested, at a heating rate of 2 °C/min. A dynamic force of 6 N was used oscillating at fixed frequency and amplitude of 30 μm.

Tensile testing was performed on an MTS 858 Table Top Servohydraulic test frame equipped with hydraulic grips. Each dog-bone coupon was placed in the grips and tested in displacement control at a loading rate of 0.050 inches/min (1.27 mm/min) to failure. A 3D digital image correlation system (Correlated Solutions Inc, Columbia, SC) comprised of two AVT Marlin cameras was used to acquire full field strain measurements in the gauge region of each coupon. The AVT Marlin cameras had a spatial resolution of 1000 pixels × 1000 pixels and provided images with a magnification of approximately 30.1 pixels/mm. For the purpose of determining elastic modulus and elongation at failure, the virtual extensometer function in Vic 3D (Correlated Solutions Inc.) was used, which allowed for displacement changes to be accurately measured in the gauge region and converted to engineering strain. In order to obtain statistically representative data, six specimens were manufactured for each sample, and those which broke beyond the gauge region were automatically discarded in further calculations. Low magnification optical microscopy was applied to the broken surface after each tensile test to verify that coupons were broken due to normal failure rather than by the existance of a superficial flaw.

Charpy impact strength measurements were carried out using a CEAST Fractovis dart impact tester. A hammer mass of 1.096 kg impacted at a constant velocity of 3.60 ms^{-1} (giving a total kinetic energy at impact of 7.10 J) on notched specimen bars with dimensions 33 × 10 × 3 mm^3, as described in the UNE-EN ISO 179 standard. Measurements were performed at 23 ± 2 °C and 50 ± 5% relative humidity. The presented data correspond to the average value of 6 - 8 specimens.

Direct current (DC) electrical conductivity was measured with a Keithley 4200-SCS source measurement unit, working at 20 V. The specimens (8.8 × 8.8 × 2.9 mm^3) were obtained from direct curing into a mold. Nanocomposite samples were placed in a sandwichlike arrangement using two copper sheets (0.2 mm thick). Measurements were carried out in a two probe configuration, with each probe placed in different 8.8 × 8.8 mm^2 square surfaces of the test sample.

AFM measurements were performed with a Multimode SPM from Veeco Instruments (Santa Barbara, US), equipped with Nanoscope V controller and JV-scanner (130μm scan size in XY, and 6μm Z-range), and placed on a passive, air-damped vibration isolation table from Technical Manufacturing Company (Boston, US). Additionally, the system included the HarmoniX option which allows acquiring force-distance curves in real time during tapping mode operation, and to extract and map mechanical properties as additional data channels.[30] Soft silicon tapping mode cantilevers with off-axis tip design and reflective backside Al-coating (tip radius 10 nm, spring constant 4 N/m, fundamental vertical resonance 70kHz, torsional resonance 1200 kHz) optimized for large bandwidth acquisition of the force distance data were used (type HMX, Veeco Probes, Camarillo, US). Probes were mounted in a cantilever holder with large dither piezo (model MFMA, Veeco Instruments, Santa Barbara, US). Tapping mode imaging set point and dither piezo drive were optimized on each sample after tip engagement by inspection of the resulting real time force distance data in such a way that about 100 nm cantilever amplitude and a peak force of about 1−5 nN was reached. Scan speed and force curve averaging was optimized to avoid undersampling (less than one force-curve per imaging pixel) and to reduce noise. Calibration of the modulus was performed by comparing the HarmoniX-data with a polymer sample of known modulus in the expected range.

3. RESULTS AND DISCUSSION

State of Dispersion. The state of dispersion was firstly controlled with optical microscopy. These observations have been performed in a blend containing TGAP and filler (prior to the hardener incorporation and curing). The obtained images (see Figure S2 in the Supporting Information) show how the solvent-free mixing protocol provides a highly homogeneous epoxy blend with no visible agglomerates in the case of Pluronic-wrapped SWNTs. In contrast, acid-treated SWNTs present a very rough and aggregated view, visibly different from that of the Pluronic-wrapped filler. In Figure 1, typical SEM and TEM images are shown for composite samples containing 0.5 wt % SWNTs (bare acid-treated and Pluronic-wrapped). In the SEM images, performed on the fractured edge of a cured test sample, the difference between the two kinds of SWNTs is evident. The incorporation of bare SWNTs acid treated into the epoxy matrix results in a visible inhomogeneity, with appreciable amounts of large domains of aggregated SWNTs (Figure 1a). The adhesion to the matrix seems to be poor because SWNTs present in the agglomerates appear to be "pulled out" intact rather than broken. When Pluronic-wrapped SWNTs are used as the reinforcement, a drastic change in the fracture edge morphology is denoted. Homogeneity in the SWNT distribution increases considerably, no agglomerates can be observed, and the thickness of SWNT bundles is greatly reduced (Figure 1b). The fracture edge overview in this case consists of SWNTs randomly oriented and broken, that appear as bright dots, indicating a very good adhesion to the matrix, as well as the possible presence of defects in the SWNT structure that enable the SWNT/matrix joint breakage. Spherical morphologies formed by the BC are more easily seen at higher filler loadings (2 wt % SWNT−Pluronic).[26]

A closer look at both samples was made by TEM, using test samples cut with a microtome. For the nanocomposite containing bare acid-treated SWNTs, large areas with no filler were observed, containing some nanometric-sized aggregates of SWNTs (Figure 1c). On the other hand, the nanocomposite containing Pluronic-wrapped SWNTs showed a different pattern wherein

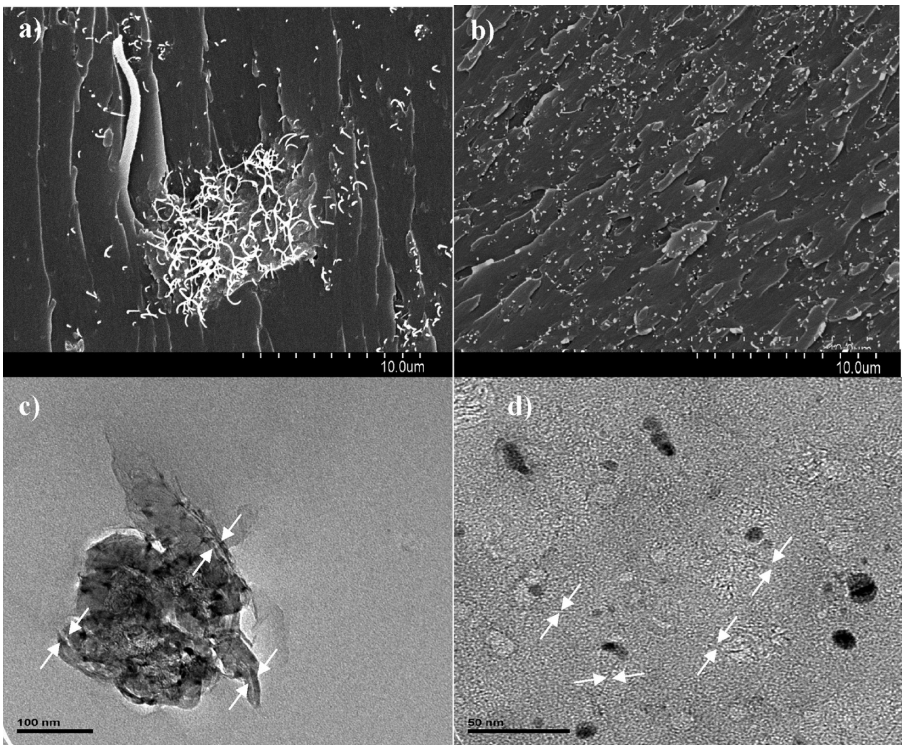

Figure 1. SEM (top) and TEM (bottom) images for the nanocomposite sample containing 0.5 wt % of filler: (a, c) bare SWNTs nanocomposites, (b, d) Pluronic-wrapped containing sample. Arrows indicate the presence of individual SWNTs.

different nanostructures formed by the BC could be seen (Figure 1d), with no evidence of aggregates. In this latter sample, SWNTs were fully embedded in the epoxy matrix and therefore barely visible, but some individual SWNTs were detected, indicating important improvements in the disentanglement and distribution of the filler inside the matrix. Optical microscopy is consistent with observations made by SEM and TEM.

Dynamical Mechanical Study. DMA over a wide temperature range is very sensitive to the physical and chemical structure of epoxy resins and their composites. A study of the storage modulus and tan δ curves is very useful in ascertaining the relaxation behavior of a sample under load and temperature. A clear understanding of the storage modulus−temperature curve obtained during DMA provides valuable insights into the stiffness of a material as well as the molecular relaxations taking place, both as a function of temperature. In Figure 2a the storage moduli data are shown for different nanocomposite and blank samples (see Figure S3 in the Supporting Information, where some examples of Storage and Loss moduli curves are depicted). Epoxy nanocomposites based on acid-treated SWNTs experience a moderate increase in the storage modulus. The reinforcing role of SWNTs in the dynamic mechanical performance of epoxy resin is controlled by the SWNT concentration. Composites with 1 wt % of acid-treated SWNTs improved the storage modulus of the epoxy resin at room temperature by 28%. The 0 wt % baseline blank represents the epoxy matrix subjected to the same mixing protocol as the rest of nanocomposite samples. The utilized procedure does not cause significant damage to the neat matrix despite the tip-sonication process. The incorporation of small amounts of Pluronic F68 BC leads to a decrease in the storage moduli of 33.5%, which is apparently independent of Pluronic concentration in the studied range. This is consistent with

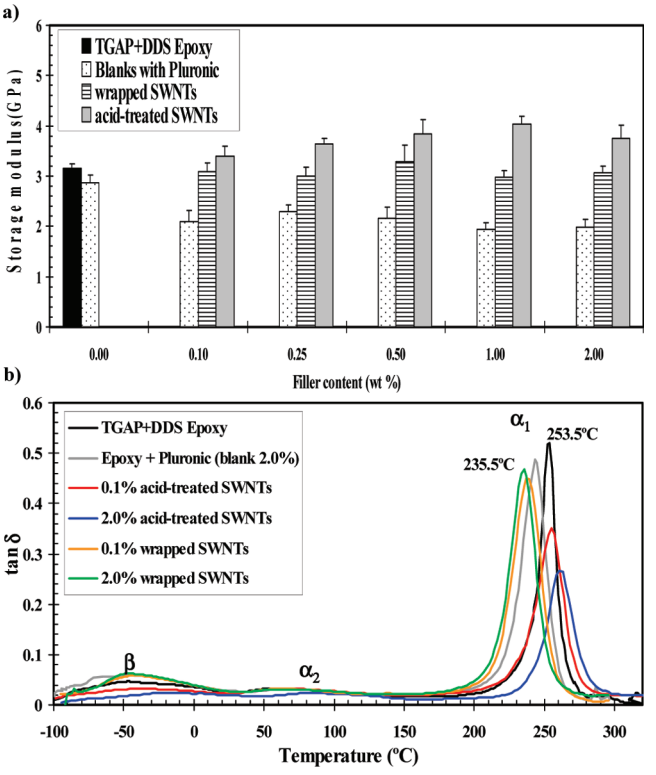

Figure 2. Dynamic mechanical analysis of epoxy nanocomposites obtained at the frequency of 1 Hz and 25°C() value of storage modulus obtained at room temperature versus filler concentration, and (b) evolution of tan δ for some different compositions of epoxy resin versus temperature at 1 Hz.

observations reported by other authors working with different epoxy matrices modified with PEO-based BCs.[31,32] This fact may be attributed to a strong plasticizing effect caused by the BC. The presence of a BC within the epoxy matrix leads to spherical nanostructure formation by self-assembly which may encapsulate epoxy material, leading to a nano-segregated feature consisting of BC and epoxy as will be shown in AFM images. The rubbery layer between the inner and outer part of the spherical nanostructures is probably weakly bonded to the epoxy, causing this plastic behavior. With regards to the addition of Pluronic-wrapped SWNTs, a large increase is observed in the storage moduli of all samples compared with their respective Epoxy + Pluronic blanks. This leads to final moduli values nearly that of the neat epoxy (Fig. 2a), with no dependence on filler concentration. As an example, the modulus increase with respect to its own blank sample for the lowest loading of Pluronic-wrapped SWNTs (0.1 wt % filler) is 0.99 GPa (an increase of 47%). This represents a large increase with a very small amount of the filler (30 wt % BC and 70 wt % SWNTs in the filler, thus 0.07 wt % of SWNTs in the composite, see Experimental Section). The reinforcement role of SWNTs seems to be enhanced when wrapped in Pluronic and this fact compensates for the plasticizing effect of the BC, leaving the final moduli values unchanged with respect to the neat matrix.

On the other hand, the damping factor (tan δ) tests allow studying glass or secondary transitions. As can be seen in Figure 2b, the resin system displays three transition peaks in the curve. The transition at the lowest temperatures is the secondary relaxation associated with the β-transition while the other relaxations are associated with different α-transition temperatures of the cured network. The α_1-transition (glass transition) can be related to Brownian motion of the main chains at the transition from the glassy to the rubbery state and the relaxation of associated dipoles, at a specific temperature (T_g). The β-transition occurs at significantly lower temperatures and it is well known to be related to crankshaft rotation of hydroxyl ether segments ($-CH_2-CH(OH)-CH_2-O-$) of the crosslinked network in the glassy state.[33] The appearance of these two α transitions related to the epoxy network, while not common, has been reported previously for high-performance structural epoxy resins possessing high functionality monomers.[34] For the sake of clarity, only the extreme compositions are shown in Figure 2b. The addition of acid-treated SWNTs leads to a progressive increase in both β and α_1 transition temperatures of the neat epoxy (initially about -50 and 253.5 °C, respectively). The height of the α_1 transition peak also progressively decreases with the addition of acid-treated SWNTs, in good agreement with an increase in the rigidity of the system. However, the α_2 transition temperature appears unchanged. Upon addition of Pluronic a reduction in T_g was found, on the order of 18°C for samples containing Pluronic-wrapped SWNTs and 10.5 °C for the Epoxy + Pluronic blank references. Furthermore, the presence of Pluronic strongly influences the α_2 transition of the neat epoxy resin. The value of the α_2 transition temperature decreased drastically with the addition of Pluronic. These facts confirm the strong plasticizing effect of Pluronic. Similar observations were reported by other authors working with Pluronic and other epoxy resins.[35] The broadening of the α_1 peak might be related to restrained chain mobility that usually occurs in compatible blends, slowing the mobility of the matrix chains, hence creating a wider temperature transition.[36] It can be assumed that molecules located close to the nanofiller possess different mobility than those fully embedded in an epoxy environment,

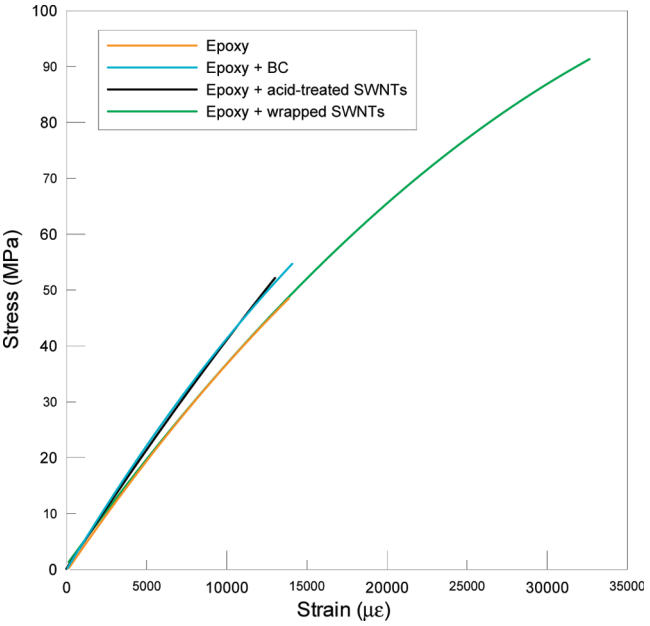

Figure 3. Representative stress−strain curves for the epoxy +0.5 wt % wrapped−SWNT nanocomposite sample and different control samples.

leading to a broadening of the relaxation peaks. Contrary to the epoxy + acid-treated SWNT samples, in the case of nanocomposites with Pluronic-wrapped SWNTs, no significant changes are observed in this parameter with respect to their corresponding blanks, suggesting that SWNTs are not able to fully develop their ability to restrict motion when wrapped in the BC.

Overall, the results provided by this technique show that the incorporation of SWNTs wrapped by this BC into the epoxy maintain the stiffness of the neat resin. The storage moduli of the samples containing Pluronic-wrapped SWNTs experience a very pronounced increase with respect to the epoxy + Pluronic blank references, independent of the filler content, while giving absolute moduli values comparable to that of the neat epoxy. Pluronic-containing samples exhibit significantly lower T_g values even with small additions of the filler.

Tensile Tests. One of the epoxy−SWNT samples was selected to carry out a series of tensile experiments. As a compromise between nanotube loading and dynamical mechanical properties, the nanocomposite with 0.5 wt % filler was chosen. Four different samples were prepared: the TGAP + DDS neat epoxy, the 0.5 wt % nanocomposite containing Pluronic-wrapped SWNTs, the blank epoxy + BC sample (with 0.15 wt % of Pluronic) and the nanocomposite sample containing 0.5 wt % of acid-treated SWNTs. In a typical tensile experiment, the stress-strain ($\sigma-\varepsilon$) curve obtained is shown in Fig. 3. The ultimate strain or elongation (ε_{max}) and ultimate tensile stress (UTS) are extracted from the curve just before the failure. Young's modulus (E) is obtained from the slope of the linear fit in the initial section of the curve (up to 5000 $\mu\varepsilon$, i.e. 0.05% strain). Finally, the toughness (G) was estimated by calculating the area under the curve using eq 1

$$G = \sum_{\varepsilon=0}^{\varepsilon_{max}} \sigma \Delta\varepsilon \qquad (1)$$

Mechanical parameters drawn from $\sigma-\varepsilon$ curves for the different samples are depicted in Figure 4. In this figure, error bars represent

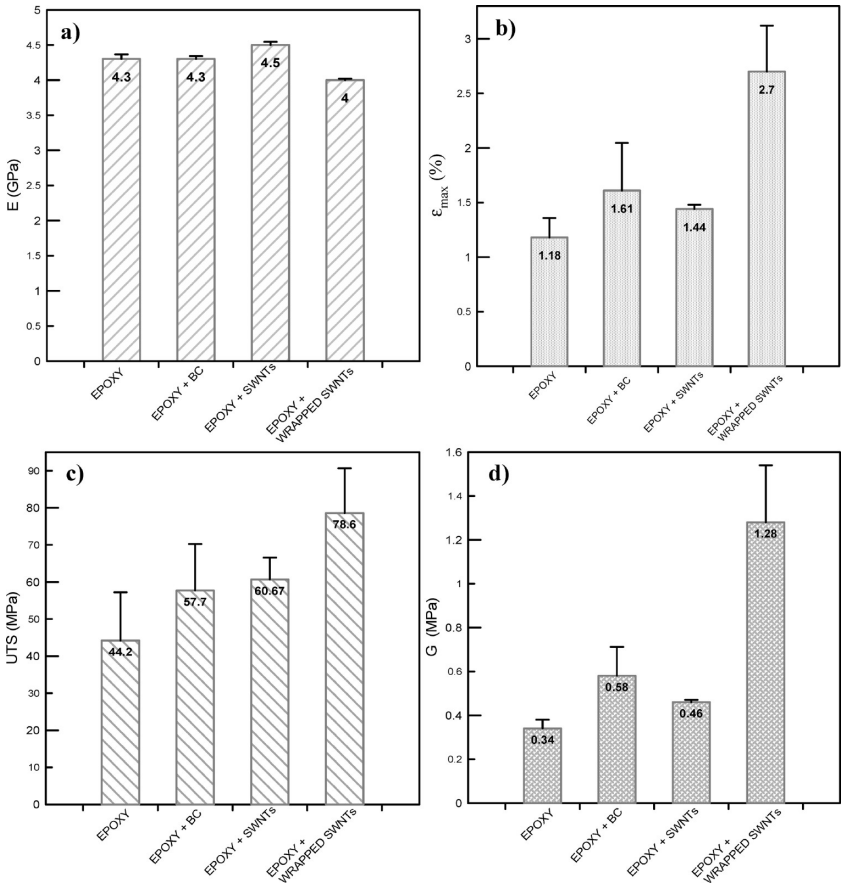

Figure 4. Mechanical parameter extracted from stress−strain curves: (a) Young's modulus, (b) maximum strain, (c) ultimate tensile strength, and (d) toughness.

confidence intervals calculated through the Student's "t-test" (statistical significance >90%). The epoxy matrix possessed a high Young's modulus value (4.3 GPa) but low toughness (0.34 MJ/m^3), as expected with an inherently brittle material. It is clear that the incorporation of acid-treated SWNTs (0.5 wt %) slightly increased the matrix Young's modulus and moderately increased toughness by 4.7% and 35% respectively. It was also found that ε_{max} decreases by 6.5% and UTS increases by 37%. The presence of the BC in the same amount as in the Epoxy + wrapped SWNTs sample (0.15 wt % BC) was found to have a more pronounced effect on toughness, resulting in an increase of 71% with respect to the neat resin. This latter is consistent with the fact that BCs are well-known to toughen epoxy matrices.[22,23] In our case, Pluronic F68 itself is causing a visible toughness improvement despite the low amounts in which it is present. Young's modulus for Epoxy + BC sample, however, remains unchanged with respect to the neat matrix, whereas ε_{max} and UTS values increase by 2.5 and 31%, respectively. Finally, for the Epoxy + wrapped SWNTs sample there was huge increase in toughness with respect to the neat matrix (276%), which is evidence for a synergistic toughening effect between SWNTs and Pluronic F68. While acid-treated SWNTs or BC do not separately cause such toughening, the combination of both (in the form of Pluronic-wrapped SWNTs) produces a remarkable toughness enhancement. This synergistic behavior was also detected for ε_{max} and UTS, which exhibit an improvement of 72 and 78%, respectively, with regard to the neat matrix, indicating a more ductile fracture behavior. The Young's modulus seems to be slightly worsened in this last case, decreasing 7.5% with respect to the neat matrix (Table S1 in the Supporting Information contains a summary of tensile parameters improvements).

Although Young's moduli enhancements in epoxy−carbon nanotube composites have extensively been reported over the past years, available toughness data in these systems are much more limited.[37] In general, extensive storage and Young's moduli enhancements have been reported in the literature but no increase or significant decrease in toughness.[6] Some few studies have shown moderate tensile toughness improvements,[7,38] but to the best of our knowledge no tensile toughness improvement comparable with the 276% found here have been demonstrated, particularly with such small amounts of filler. In addition to this, the classical methods to toughen epoxy matrices usually sacrifice other mechanical properties.[39] The mechanical data reported here shows how to selectively enhance toughness and maximum strain of an epoxy resin with virtually no change in other mechanical properties. The BC-wrapping provides epoxy-miscible filler with excellent toughening properties while, in contrast, a moderate increase in storage moduli and tensile properties can be achieved by solvent-free dispersion of acid-treated SWNTs.

The incorporation of a BC into an epoxy matrix in the form of BC-wrapped SWNTs would provide enhanced surface area and thus the intrinsic BC toughening effect could be boosted. The BC is strongly bound to the SWNTs during the wrapping process,

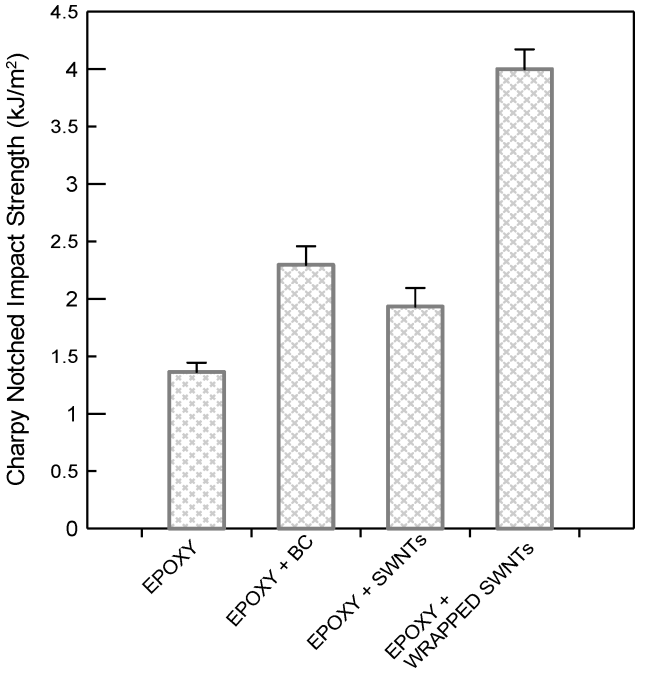

Figure 5. Room temperature notched impact toughness of the neat epoxy matrix, the composite containing 0.5 wt % Pluronic-wrapped SWNTs and the corresponding reference composites.

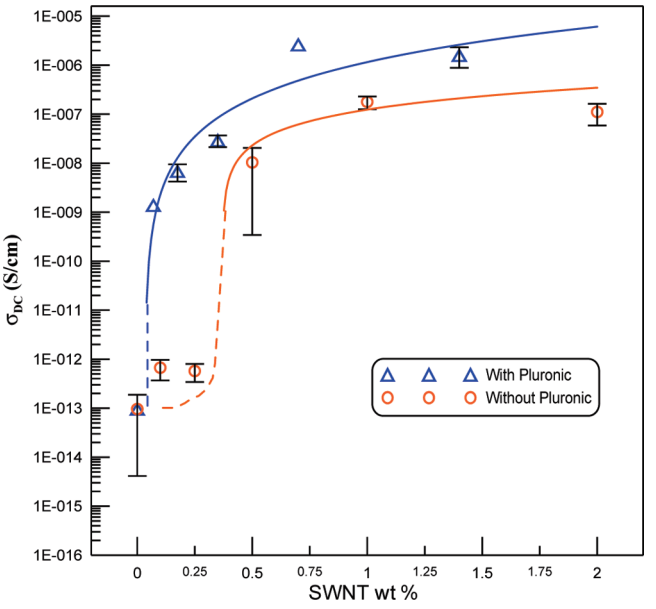

Figure 6. Electrical conductivity vs SWNTs actual content for samples containing acid treated and Pluronic-wrapped SWNTs. Solid lines correspond to the percolation theory fitting. Dashed lines provide additional visual aid.

thanks to the van der Waals forces, polar interactions between oxygen groups in both BC and SWNTs, and by a noticeable steric stabilization. It could be assumed that the interface between BC-wrapped SWNTs and the matrix is ruled by the interactions between the wrapping BC and the epoxy. The chemical similarity and miscibility, but nonreactivity of PEO with the target matrix allows interfacial bonding throughout polar interactions (dipole forces) and the possible existence of hydrogen bonds (i.e., between PEO ethers and epoxy's unreacted OHs). The PPO block would remain more strongly bound to the SWNTs than PEO within the epoxy environment, being jointly responsible of the interfacial connection of the filler with the matrix. Recent studies about the adsorption and self-assembly of Pluronic block copolymers on SWNTs[40] report the formation of new hybrid SWNT−polymer elongated-micelle-like structures where a SWNT is located at the core of the cylindrical aggregate. According to these studies, it seems feasible that the presence of SWNTs would hinder the typical spherical micellation within the epoxy matrix, favoring the formation of micrometer-long cylindrical aggregates with increased surface areas which would be more efficient in toughening the epoxy matrix. This could be an explanation for the huge toughness increase reported herein.

Charpy Impact Strength. To further characterize the toughness of the composites, room temperature Charpy notched impact strength measurements were carried out, and the results are shown in Figure 5. The impact strength of the pure resin is around 1.4 kJ/m^2 and increases by about 66% for the blank sample, with Pluronic, because of the toughening effect of the BC which increases the flexibility of the epoxy. Acid-treated SWNTs lead to a moderate increase in the impact strength (∼41% at 0.5 wt % SWNT content), whilst for composites incorporating the same amount of Pluronic-wrapped nanofillers, the increase was exceptionally higher (193%), in accordance with that observed in toughness obtained from tensile data. This unprecedented toughness enhancement is ascribed to a strong increase in the energy dissipated, because of the synergistic effect between SWNTs and the BC. This percentage improvement in Charpy impact strength, to the best of our knowledge, is considerably higher than the best found in the literature, which were achieved by covalent integration of aminated multi-walled carbon nanotubes into DGEBA-based epoxy systems.[41−44] The impact strength results can be correlated with the dynamic mechanical properties in terms of the area under the loss peaks (tan δ), because it is representative of the energy dissipated in the viscoelastic relaxations. Any molecular process which promotes energy dissipation, would enhance the impact resistance of the polymer.[45] Composites with Pluronic-wrapped SWNTs present considerably larger area under tan δ peak (Fig. 2b), hence are able to dissipate more energy than those reinforced with acid-treated fillers. The results provided by the different mechanical tests indicate that the addition of Pluronic (particularly in the form of wrapped SWNTs) reduces the detriment in energy dissipation caused by the incorporation of the stiff nanotubes, thereby leading to a huge improvement in the toughness of the composites.

Electrical Conductivity. Figure 6 shows electrical conductivity measurements for all the samples prepared in this study. DC conductivity values are presented versus SWNT content, which is dependent on the presence or absence of Pluronic BC. According to the final Pluronic content in the Pluronic-wrapped SWNTs (see Experimental Section) the SWNT wt % was recalculated for the series of samples containing Pluronic. Conductivity values are higher when using Pluronic-wrapped SWNTs as the reinforcement, particularly at low loading. Samples without Pluronic do not show a substantial increase in conductivity with increasing content of SWNT until 0.5 wt % (∼1 × 10^{-7} S/cm). However, Pluronic containing nanocomposites reach the highest conductivity values at lower SWNT wt % (1−2 wt % wrapped SWNTs, equivalent to 0.7−1.4 wt % of

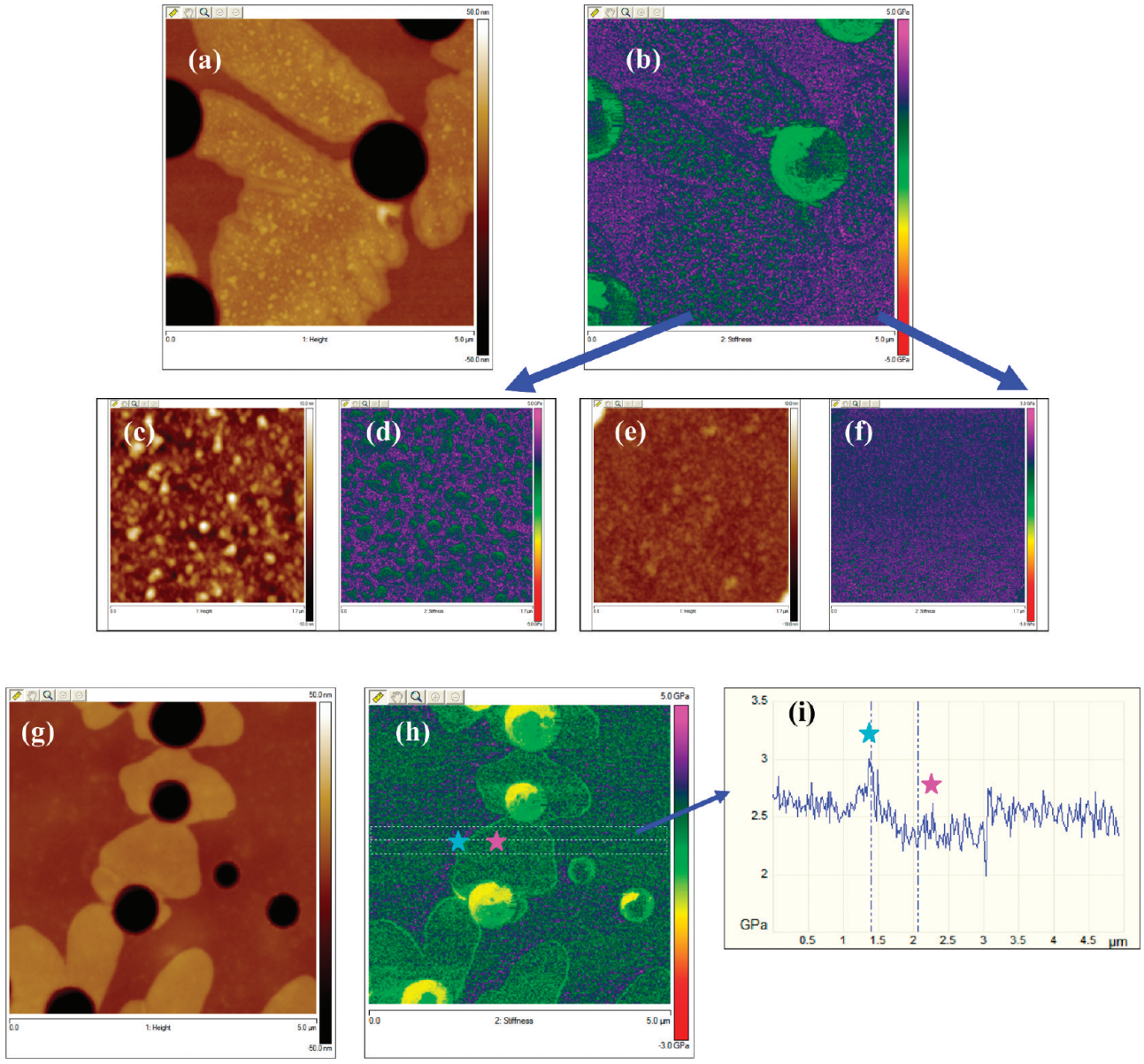

Figure 7. Topography images (a, c, e, and g) and stiffness maps (b, d, f, and h) for two samples: (a, b) Epoxy + Pluronic (0.6%) sample; (c, d) high-resolution scan of the patch area in Figure 6a,b; (e, f) high-resolution scan of the area between patches in Figure 6a,b; (g, h) Epoxy +2 wt % Pluronic-wrapped SWNTs sample; (i) averaged cross-section profile along the line in Figure 6h.

bare acid-treated SWNTs). The latter samples achieve conductivity values increased by about 7 orders of magnitude (with respect to the neat matrix) with a relatively low effective amount of SWNTs (<1 wt %).

Considering the percolation threshold defined by the universal percolation law[46] (where, for $p > p_c$, conductivity is proportional to the $(p - p_c)^t$ factor) the application of percolation theory to both series of samples provides significantly different results. Conductivity values in both cases follow a similar trend, which can be fitted to the aforementioned scaling law (Figure 6, solid lines) but with very different threshold (p_c) values. For Pluronic-wrapped SWNT nanocomposites, an approximate percolation threshold of 0.03 wt % can be derived from curve fitting (with t = 2.35), whereas a value of 0.31 wt % is obtained for bare acid-treated SWNT nanocomposites (t = 1.1). The series of samples with Pluronic-wrapped SWNTs reached the electrical percolation threshold at the lowest filler loading, 0.1 wt % of Pluronic-wrapped SWNTs, exhibiting a very sharp conductivity increase to 0.14×10^{-8} S/cm. This conductivity represents an increase of 4.1 orders of magnitude with respect to the neat matrix, achieved with a very low effective content of SWNTs (0.07 wt %) and a corresponding associated amount of BC (0.03 wt %). This is comparable to the remarkable data reported by Liu et al.[47] who achieved an increase of 4.3 orders of magnitude in electrical conductivity by incorporating clay-dispersed SWNTs (0.05 wt % SWNTs and 0.2 wt % clay) into an epoxy matrix.

In our system, it is necessary to go beyond 0.25 wt % of bare acid-treated SWNTs in the binary composites to achieve the percolation threshold. The nitric acid purification applied (see Experimental Section) promotes SWNT compaction (manifested by a drastic reduction in the specific surface area[48]), becoming an obstacle to solvent-free dispersion into the epoxy matrix. This

would explain the high percolation threshold and lower overall conductivity values. This latter data are also in agreement with the fact that chemically treated (in this case, oxidized) nanotubes show higher percolation thresholds, because of the functionalization process[49] that induces disruption of the conjugated electronic structure as well as length cutting (lower aspect ratio) of the nanotubes. In fact, this kind of oxidative treatment has been reported as one of the most harmful for electrical conductivities in epoxy nanocomposites.[50,51] It has been previously stated[52] that in a given epoxy system, there is a critical SWNT aspect ratio value above which nanotubes disentanglement at the nanoscale and the uniform distribution of individual nanotubes in the matrix are critical issues. Below this limit, percolation threshold tends to increase rapidly with decreasing aspect ratio. Therefore, Pluronic wrapping on acid-treated SWNTs counteracts this effect.

Electrical conductivity measurements show how the Pluronic-wrapping dispersion method induces a more pronounced enhancement of properties (compared to acid-treated SWNTs), particularly at the lowest loadings. This can be ascribed to the highly homogeneous distribution of disentangled SWNTs across the matrix. Additionally there is a reduction of the needed amount of SWNTs to cause such improvements because of the presence of BC.

Atomic Force Microscopy (AFM) Stiffness Characterization. In Figure 7, topography and stiffness images are shown for two epoxy samples: epoxy + 0.6 wt % Pluronic and epoxy + 2 wt % Pluronic-wrapped SWNTs. Topography views (Figure 7a, c, e, g) depict the morphological features observed. The neat epoxy matrix (not shown) has a very smooth and regular surface. Incorporation of 0.6 wt % Pluronic leads to the formation of surface holes and a "peak−valley" topographic profile resulting from the BC micellar or vesicular nanostructures. The appearance of elevated patch areas next to deep valleys is observed as a consequence of this nanostructure formation (Figure 7a). The incorporation of Pluronic-wrapped SWNTs shows similar overall topographic features as the epoxy + Pluronic sample, with the formation of deep surface holes surrounded by patch areas, although with both features in smaller areas, and with less pronounced nanostructures (Figure 7g).

The AFM stiffness investigation indicates that the neat epoxy possesses a very homogeneous profile (not shown), with high stiffness (∼3 GPa). The patches formed upon Pluronic addition (0.6 wt %) exhibit in average a lower stiffness (∼2.6 GPa, Figure 7d), while the areas between patches (Figure 7e, f) correspond to a stiffness closer to the neat matrix (∼2.8 GPa, Figure 7f).

The patch region seems to be a Pluronic-rich phase and experiences nanoscale separation into two components with different stiffness. A more detailed analysis of the patch region via averaged line profiling (not shown, but analogous to Figure 7i) reveals that the softer component has a stiffness of about 2.2 GPa, whereas the stiffer component is similar to the neat matrix (again ∼2.8 GPa).

Addition of SWNTs (2 wt % Pluronic-wrapped) affects both the patch area and the area between the patches: the patch area becomes smaller, softer (overall similar to the soft component in the patches on the epoxy + Pluronic sample, ∼2.3 GPa) and more homogeneous, as shown in Figures 7g and 7h.

In contrast to the patch area, now two more-or-less homogeneous phases coexist in the area between the patches (Figure 7h). One of these phases has comparable stiffness and surface structure to that of the neat epoxy; the other one has a stiffness value close to the average over the patch area on the epoxy + Pluronic sample. However, the latter phase is not identical to the patches in Figure 6b, as can be concluded from the difference in the nanostructure.

The three phases identified on this sample are discernible both in the imaged cross-section (Figure 7i) and in the stiffness map (Figure 7h). It seems that, on the sample with 2 wt % Pluronic wrapped-SWNTs, the stiffest region forms some sort of band around the two softer regions.

AFM stiffness correlates with that obtained through the DMA technique. The neat epoxy matrix exhibits a stiffness value corresponding to its storage modulus (Figure 2a). The epoxy + Pluronic sample has a storage modulus of about 2 GPa, in good agreement with the AFM stiffness value, in particular with that of the nanostructured features contained within the patches. These nanostructures would dominate the macroscopic mechanical behavior of this sample. In contrast, for Pluronic-wrapped samples containing SWNTs, the storage modulus (3 GPa) corresponds to the stiffness of the phase surrounding the patches, and is comparable to the neat matrix. In this case, this phase dominates the macroscopic mechanical behavior. Thus, the influence of Pluronic and Pluronic-wrapped SWNTs on the dynamical mechanical properties was reasserted with the AFM measurements.

4. CONCLUSIONS

A noncovalent dispersion strategy based on SWNT wrapping by a PEO-based block copolymer (Pluronic F68) has successfully been applied to a high-performance epoxy resin. The Pluronic-wrapped SWNTs exhibited high miscibility in the epoxy matrix as compared with nitric acid-treated SWNTs, enabling successful dispersion without the use of solvents. As-prepared nanocomposite materials had an enhanced distribution and more homogeneous dispersion of the filler within the epoxy matrix when incorporating Pluronic-wrapped SWNTs as compared to bare acid-treated SWNTs, which tend to severely agglomerate. Characterization of both types of nanocomposite materials reveals that epoxy composites containing Pluronic-wrapped SWNTs exhibit significant improvements in mechanical properties (i.e., 276% improvement in toughness or 193% improvement in impact strength with respect to the neat epoxy matrix for 0.5 wt % of SWNT−Pluronic nanocomposite,) while leaving elastic modulus practically unchanged, and with no dependence on the filler concentration in the studied range. The incorporation of bare acid-treated SWNTs resulted in a modest improvement of the overall mechanical performance, which was dependent on the nanotube content. DMA data are supported by AFM stiffness mappings, in which relative stiffness of the different phase morphologies of epoxy−Pluronic−SWNTs are studied. Electrical conductivity measurements showed higher values in all cases for SWNT−Pluronic nanocomposites with a percolation threshold about ten-fold lower than bare acid-treated SWNTs nanocomposites. With Pluronic-wrapped SWNTs, the matrix electrical conductivity was increased by around 7 orders of magnitude at a relatively low filler content (less than 1 wt %). A synergistic effect between SWNTs and the block copolymer is therefore suggested, given that these improvements are higher than a simple sum of individual effects. The reinforcement potential of Pluronic-wrapped SWNTs is therefore demonstrated herein, and the utility of this approach allows enhancing the dispersion of hardly dispersible carbon nanotubes in epoxy matrices, such as nitric

acid-treated, without using organic solvents and allows for large improvements in the physical properties with smaller effective amounts of SWNTs.

■ ASSOCIATED CONTENT

Supporting Information. Raman spectra of the different SWNTs, optical images of SWNT dispersion in the epoxy, and different storage and loss moduli curves of the epoxy composites. This material is available free of charge via the Internet at http://pubs.acs.org/.

■ AUTHOR INFORMATION

Corresponding Author
*E-mail: mtmartinez@icb.csic.es.

■ ACKNOWLEDGMENT

The authors thank financial support from the NRC (Canada) − CSIC (Spain) collaboration project and also thank Huntsman company. Mr. González-Domínguez gratefully acknowledges the Spanish Ministry of Innovation (MICINN) for his FPU predoctoral grant. Special thanks to Mercedes Vico at the Instituto de Carboquimica (Spain) for her helpful assistance

■ REFERENCES

(1) Coleman, J. N.; Khan, U.; Gun'ko, Y. *Adv. Mater.* **2006**, *18* 689–706.
(2) Thostenson, E. T.; Ren, Z. F.; Chou, T. W. *Compos. Sci. Technol.* **2001**, *61*, 1899–1912.
(3) Moniruzzaman, M.; Winey, K. I. *Macromolecules* **2006**, *39* 5194–5205.
(4) Jung, Y. C.; Shimamoto, D.; Muramatsu, H.; Kim, Y. A.; Hayashi, T.; Terrones, M.; Endo, M. *Adv. Mater.* **2008**, *20*, 4509–4512.
(5) Jung, Y. C.; Muramatsu, H.; Park, K. C.; Shimamoto, D.; Kim, J. H.; Hayashi, T.; Song, S. M.; Kim, Y. A.; Endo, M.; Dresselhaus, M. S. *Macromol. Rapid Commun.* **2009**, *30*, 2084–2088.
(6) Coleman, J. N.; Khan, U.; Blau, W. J.; Gun'ko, Y. K. *Carbon* **2006**, *44*, 1624–1652.
(7) Gojny, F. H.; Wichmann, M. H. G.; Köpke, U.; Fiedler, B.; Schulte, K. *Compos. Sci. Technol.* **2004**, *64*, 2363–2371.
(8) Guo, P.; Chen, X.; Gao, X.; Song, H.; Shen, H. *Compos. Sci. Technol.* **2007**, *67*, 3331–3337.
(9) Zhu, J.; Kim, J. D.; Peng, H.; Margrave, J. L.; Khabashesku, V. N.; Barrera, E. V. *Nano Lett.* **2003**, *3*, 1107–1113.
(10) Zhang, W.; Srivastava, I.; Zhu, Y. F.; Picu, C. R.; Koratkar, N. A. *Small* **2009**, *5*, 1403–1407.
(11) Cui, S.; Canet, R.; Derre, A.; Couzi, M.; Delhaes, P. *Carbon* **2003**, *41*, 797–809.
(12) Geng, Y.; Liu, M. Y.; Li, J.; Shi, X. M.; Kim, J. K. *Composites: Part A* **2008**, *39*, 1876–1883.
(13) Gong, X.; Liu, J.; Baskaran, S.; Voise, R. D.; Young, J. S. *Chem. Mater.* **2000**, *12*, 1049–1052.
(14) Pécastaings, G.; Delhaes, P.; Derre, A.; Saadaoui, H.; Carmona, F.; Cui, S. *J. Nanosci. Nanotechnol.* **2004**, *4*, 838–843.
(15) Wang, S.; Liang, Z.; Gonnet, P.; Liao, Y. H.; Wang, B.; Zhang, C. *Adv. Funct. Mater.* **2007**, *17*, 87–92.
(16) Graff, R. A.; Swanson, J. P.; Barone, P. W.; Baik, S.; Heller, D. A.; Strano, M. S. *Adv. Mater.* **2005**, *17*, 980–984.
(17) Grady, B. P. *Macromol. Rapid Commun.* **2010**, *31*, 247–257.
(18) Lau, K. T.; Lu, M.; Lam, C.; Cheung, H.; Sheng, F. L.; Li, H. L. *Compos. Sci. Technol.* **2005**, *65*, 719–725.
(19) Li, Q.; Zaiser, M.; Koutsos, V. *Phys. Status Solidi, A* **2004**, *201*, R89–R91.
(20) Cho, J.; Daniel, I. M. *Scr. Mater.* **2008**, *58*, 533–536.
(21) Cho, J.; Daniel, I. M.; Dikin, D. A. *Composites, Part A* **2008**, *39*, 1844–1850.
(22) Ruiz-Pérez, L.; Royston, G. J.; Fairclough, P. A.; Ryan, A. J. *Polymer* **2008**, *49*, 4475–4488.
(23) Ruzette, A. V.; Leibler, L. *Nat. Mater.* **2005**, *4*, 19–31.
(24) Schvartzman-Cohen, R.; Nativ-Roth, E.; Levi-Kalisman, Y.; Yeruzalmi-Rozen, R. *Langmuir* **2004**, *20*, 6085–6088.
(25) González-Domínguez, J. M.; Castell, P.; Ansón, A.; Maser, W. K.; Benito, A. M.; Martinez, M. T. *J. Nanosci. Nanotechnol.* **2009**, *9*, 6104–6112.
(26) González-Domínguez, J. M.; Ansón-Casaos, A.; Castell, P.; Díez-Pascual, A. M.; Gómez, M. A.; Martinez, M. T. *Polym. Degr. Stab.* **2010**, *95*, 2065–2075.
(27) Journet, C.; Maser, W. K.; Bernier, P.; Loiseau, A.; Lamy de la Chapelle, M.; Lefrant, S.; Deniard, P.; Lee, R.; Fischer, J. E. *Nature* **1997**, *388*, 756–758.
(28) Montesa, I.; Muñoz, E.; Benito, A. M.; Maser, W. K.; Martínez, M. T. *J. Nanosci. Nanotechnol.* **2007**, *17*, 3473–3476.
(29) *ASTM D638. Standard Test Method for Tensile Properties of Plastics*; ASTM International: West Conshohocken, PA, 2008.
(30) Sahin, O.; Erina, N. *Nanotechnology* **2008**, *19*, 445717.
(31) Dean, J. M.; Grubbs, R. B.; Saad, W.; Cook, R. F.; Bates, F. S. *J. Polym. Sci. B: Polym. Phys.* **2003**, *41*, 2444–2456.
(32) Dean, J. M.; Lipic, P. M.; Grubbs, R. B.; Cook, R. F.; Bates, F. S. *J. Polym. Sci. B: Polym. Phys.* **2001**, *39*, 2996–3010.
(33) Yi, F.; Zheng, S.; Liu, T. *J. Phys. Chem B* **2009**, *113*, 1857–1868.
(34) Varley, R. J.; Hodgkin, J. H.; Simon, G. P. *Polymer* **2001**, *42*, 3847–3858.
(35) Larrañaga, M.; Serrano, E.; Martin, M. D.; Tercjak, A.; Kortaberria, G.; de la Caba, K.; Riccardi, C. C.; Mondragón, I. *Polym. Int.* **2007**, *56*, 1392–1407.
(36) Lin, M. S.; Lee, S. T. *Polymer* **1997**, *38*, 53–58.
(37) Spitalsky, Z.; Tasis, D.; Papagelis, K.; Galiotis, C. *Progr. Polym. Sci.* **2010**, *35*, 357–401.
(38) Gojny, F. H.; Wichmann, M.; Köpke, M.; Fiedler, B.; Schulte, K. *Compos. Sci. Technol.* **2005**, *65*, 2300–2313.
(39) Johnston, N. J. *Toughened Composites*; Special Technical Publication 937; ASTM International: West Conshohoken, PA, 1987.
(40) Shvartzman-Cohen, R.; Monje, I.; Florent, M.; Frydman, V.; Goldfarb, D.; Yerushalmi-Rozen, R. *Macromolecules* **2010**, *43*, 606–614.
(41) Wang, J.; Fang, Z.; Gu, A.; Xu, L.; Liu, F. *J. Appl. Polym. Sci.* **2006**, *100*, 97–104.
(42) Yang, K.; Gu, M.; Guo, Y.; Pan, X.; Mu, G. *Carbon* **2009**, *47*, 1723–1737.
(43) Li, S. Q.; Wang, F.; Wang, Y.; Wang, J. W.; Ma, J.; Xiao, J. *J. Mater. Sci.* **2008**, *43*, 2653–2658.
(44) Byun, J.; Kim, D. S. *Polym. Compos.* **2010**, *31*, 1449–1456.
(45) Jafari, S. H.; Gupta, A. K. *J. Appl. Polym. Sci.* **2000**, *78*, 962–971.
(46) Stauffer, D.; Aharony, A. In *Introduction to Percolation Theory*; Taylor & Francis: London, 1994.
(47) Liu, L.; Grunlan, J. C. *Adv. Funct. Mater.* **2007**, *17*, 2343–2348.
(48) Martinez, M. T.; Callejas, M. A.; Benito, A. M.; Maser, W. K.; Cochet, M.; Seeger, T.; Anson, A.; Schreiber, J.; Gordon, C.; Marhic, C.; Chauvet, O.; Fierro, J. L. G. *Carbon* **2003**, *41*, 2247–2256.
(49) Gojny, F. H.; Wichmann, M. H. G.; Fiedler, B.; Kinloch, I. A.; Bauhofer, W.; Windle, A. H.; Schulte, K. *Polymer* **2006**, *47*, 2036–2045.
(50) Kim, Y. J.; Shin, T. S.; Choi, H. D.; Kwon, J. H.; Chung, Y. C.; Yoon, H. G. *Carbon* **2005**, *43*, 23–30.
(51) Spitalsky, Z.; Krontiras, C. A.; Georga, S. N.; Galiotis, C. *Composites, Part A* **2009**, *40*, 778–783.
(52) Li, J.; Ma, P. C.; Chow, W. S.; To, C. K.; Tang, B. Z.; Kim, J. K. *Adv. Funct. Mater.* **2007**, *17*, 3207–3215.